

Copyright © 1987, by the author(s).
All rights reserved.

Permission to make digital or hard copies of all or part of this work for personal or classroom use is granted without fee provided that copies are not made or distributed for profit or commercial advantage and that copies bear this notice and the full citation on the first page. To copy otherwise, to republish, to post on servers or to redistribute to lists, requires prior specific permission.

TRANSIENT ELECTROSTATIC POTENTIALS DRIVEN BY
SHORT-PULSE ELECTRON CYCLOTRON HEATING

by

A. J. Lichtenberg, M. A. Lieberman and R. H. Cohen

Memorandum No. UCB/ERL M87/17

20 February 1987

COVER PAGE

x
TRANSIENT ELECTROSTATIC POTENTIALS DRIVEN BY
SHORT-PULSE ELECTRON CYCLOTRON HEATING

by

A. J. Lichtenberg, M. A. Lieberman and R. H. Cohen

x
Memorandum No. UCB/ERL M87/17

20 February 1987

x
ELECTRONICS RESEARCH LABORATORY

College of Engineering
University of California, Berkeley
94720

TITLE PAGE

TRANSIENT ELECTROSTATIC POTENTIALS DRIVEN BY
SHORT-PULSE ELECTRON CYCLOTRON HEATING

by

A. J. Lichtenberg, M. A. Lieberman and R. H. Cohen

Memorandum No. UCB/ERL M87/17

20 February 1987

ELECTRONICS RESEARCH LABORATORY

College of Engineering
University of California, Berkeley
94720

Transient Electrostatic Potentials Driven by Short-Pulse Electron Cyclotron Heating

A. J. Lichtenberg and M. A. Lieberman

Department of Electrical Engineering and Computer Sciences
and the Electronics Research Laboratory
University of California, Berkeley, Ca 94720

R. H. Cohen

Lawrence Livermore National Laboratory
Livermore, CA 94550

Abstract

We consider electrons heated in a local resonance zone of a magnetic well created either by a linear mirror or a finite aspect ratio torus. If the heating has sufficient strength to drive a significant non-isotropy in the electron distribution function, an electrostatic potential variation along a field line is developed to maintain charge neutrality. We determine analytically the buildup of this space varying potential for times shorter than ion transit times, and find a limit to the number of electrons within the well that can be heated. We also determine the subsequent evolution of the potential on ion transit and collision time scales. The theory is applied both to large mirror ratio devices characteristic of magnetic mirror confinement and to small mirror ratio devices characteristic of Tokamaks. In the former configuration the theory is compared to experimental observations of potential build-up and decay in the MMX device and shown to be consistent with the experiments. In the latter configuration, using the expected parameters of the MTX experiment it is found that $\Delta\Phi \sim 0.3 T_e$ is built up on the hot-electron-transit time scale, dropping to about $0.2 T_e$ on the ion-transit time scale, and then decaying further on a collisional time scale. Here T_e is the electron temperature before heating. The potential has both poloidal and toroidal variation. Possible consequences include enhanced neoclassical transport and ion heating, and parametric excitation of low-frequency modes.

I. Introduction

The role of electron cyclotron resonance heating (ECRH) in creating a non-equilibrium, anisotropic, hot electron distribution and thereby creating potentials which affect other plasma species, is well known. This process is used as part of the overall mechanism in a tandem mirror for creating a potential barrier to the flow of warm electrons.¹ In this configuration the potential is the desired result and steps must be taken to prevent the natural tendency of the plasma to collisionally relax to a configuration in which the potentials are much smaller. In other situations the potentials are the inadvertent consequence of the heating process in which the hot-electron distribution is created for other reasons. These potentials may influence the heating, itself, or the transport, in ways that are sometimes deleterious to the overall operation of the device. The EBT² and the RFC-XX³ are examples of devices employing ECRH heating in which the potentials are inadvertent consequences of the heating. In the RFC-XX, for example, the heating is not azimuthally symmetric and is thought to be the source of radial $E \times B$ drifts and thus enhanced radial diffusion.³ ECRH in a tokamak is inherently non-azimuthally symmetric and would thus also give rise to radial drifts. There are other circumstances in which the resultant potentials may be beneficial, as will be discussed below.

Short-pulse ECRH, in which heating occurs on a time scale short compared to that of collisional processes, tends to give rise to large anisotropies and thus large induced potentials. In particular, on time scales during which the ions cannot move very high potentials are possible, which can have profound effects on the heating, itself. Short-pulse ECRH has been employed in a multiple-mirror experiment (MMX) in which potential barriers are created for the purpose of investigating trapped particle modes.⁴ The potentials have also been measured using a new type of electron beam, time-of-flight, potential diagnostic. The potential measurements were, in turn, used to study the transient dynamics of the various plasma species after the heating pulse.⁵ The details of the heating process and build-up of the potential were not considered, being replaced by the simplest assumption of a uniform heating of the electron distribution. High intensity short-pulse ECRH is also planned for Tokamak experiments such as MTX.⁶ In this device, also, both the short and longer time-scale potentials may affect the operation of the experiment and should therefore be considered.

In this work we consider the transient potentials associated with short-pulse ECRH, applicable both to magnetic mirror devices and to tokamaks. We will reconsider the conclusions of our previous experimental study⁵ in the light of our new viewpoint. We also will consider the effect of the potentials on the proposed tokamak experiment MTX employing short-pulse ECRH. The basic mechanism which we consider is the following: Electrons are heated in resonance zones to form a nonuniform (sloshing) density distribution $n_h(z,t)$. To preserve charge neutrality, the unheated (cold) electron density is $n_c(z,t) = n_i - n_h(z,t)$, where n_i is the background ion density. Assuming a Boltzmann cold electron distribution, a (negative) potential forms: $\Delta\Phi(z,t) = T_e \ln[n_c(z,t)/n_i]$. Both n_h and Φ build up to steady state values $n_{hs}(z)$ and $\Phi_s(z)$ on the cold electron transit timescale. Since n_{hs} cannot significantly exceed n_i , not all electrons can be heated on this timescale. On an ion transit timescale, ions move into the potential well, modifying n_h and Φ . Further modifications of n_h and Φ are on an ion or hot electron thermalization timescale.

The width of the resonance zone is a key parameter in determining the fraction of the cold electrons that can be heated before the potential buildup excludes the remaining electrons. This width may be determined either by the natural resonance width over which electrons can be heated, or by the parallel energy distribution of the unheated electrons which determines, for a given perpendicular energy gain, the spread in resonance turnings after passing through the exact resonance. The former is a property of the nonlinear dynamics of the heating, independent of the initial distribution, and is important in the strong heating limit when the final energy is orders of magnitude larger than the initial energy. The latter is a property of the distribution function of the unheated electrons and is most important when the final energy does not greatly exceed the initial energy.

For the development in the Sec. II we first take the width of the resonance zone to be a given parameter, and, using some simplifying assumptions, we determine the equilibrium hot and background electron distributions. A simple physically reasonable estimate is also made for the buildup time of this equilibrium. We then consider some experiments of interest to estimate the widths of the resonance regions, heating, and expected electron equilibrium distributions. We shall see that in the case of weak mirrors and fairly high initial electron temperature, characteristic of short-pulse heating in Tokamaks, the initial and final velocity distribution functions determine the resonance width. In Sec. III we make

a more detailed calculation, assuming that the hot-electron velocity distribution is an anisotropic Maxwellian. The calculations are then applied to the proposed short-pulse ECRH tokamak heating experiment MTX. In Sec. IV we examine the longer-time effect associated with ion motion. Then, in Sec. V we re-examine the assumptions of the MMX potential-measuring experiment within the context of our present theory. Because the final energies are orders of magnitude larger than the low initial energy, the natural resonance width is used in the calculation. In Sec. VI we apply the theory to the MTX tokamak. In Sec. VII we discuss some further implications of our work.

II. Model for the Potential

In this section we make the simplest set of physically reasonable assumptions for calculating the equilibrium potential and its buildup rate. In the next section we redo the calculation using an explicit anisotropic Maxwellian distribution for the hot electrons.

We make the following assumptions:

1. There is initially a uniform density of ions and electrons, $n_i(t = 0, s) = n_e(t = 0, s) = n_0 = \text{const}$, and the ion distribution remains fixed.
2. There is a parabolic field $B(x) = B_0 \left[1 - \frac{s^2}{L^2} \right]$.
3. The ECRH resonance zone, where electrons are heated and reflected, lies between $s = l$ and $s = l+w$, where l is the position of exact resonance, and $w \ll l$.
4. The ECRH pulse is sufficiently long that the cold electrons form a Boltzmann distribution along the magnetic field lines in response to the potential.
5. The ECRH pulse is sufficiently long that the hot electrons make enough transits to form a quasi-steady-state distribution (required only for buildup rate calculation).
6. The hot electrons are not affected by the potential.

If we assume a fraction η of the total electrons in the mirror region within l are heated and turning within $[l, l+w]$, then the incremental density within the parabolic mirror for turning between s_1 and $s_1 + ds_1$ is

$$dn_h(s, s_1) = \frac{R \eta n_i ds_1}{\pi(s_1^2 - s^2)^{1/2}}, \quad (1)$$

where $R(s) = B(s)/B_r$, and B_r is the value of B at resonance ($s=l$). Integrating over the range of turnings we have the hot electron density profile

$$n_h = \frac{\eta n_i l}{\pi w} S(s) \quad (2a)$$

where

$$S(s) = R(s) \begin{cases} \cosh^{-1} \frac{l+w}{s}, & l < s < l+w, \\ \left[\cosh^{-1} \frac{l+w}{s} - \cosh^{-1} \frac{l}{s} \right], & 0 < s < l, \end{cases} \quad (2b)$$

The hot-electron density from (2) is sketched in Fig. 1(a).

Assuming quasineutrality, $n_e = n_i$, the cold electrons within the ECRH cell form a Boltzmann distribution along the field lines in the self-consistent negative potential given by

$$\frac{\Phi(s) - \Phi(0)}{T_e} = \ln \left[\frac{n_i - n_h(s)}{n_i - n_h(0)} \right] \quad (3)$$

where "0" refers (conveniently, for mirrors) to the bottom of the well and where T_e is the background "cold" electron temperature. Φ has a logarithmic singularity at $n_h(l) = n_i$, as shown in Fig. 1(b). Clearly no cold electrons can penetrate to this position and the heating stops. At this point the fraction of cold electrons heated is, from (1) and (2),

$$\eta_m = \pi(w/2l)^{1/2}. \quad (4)$$

If we further assume that the hot electrons are sufficiently energetic compared to the cold electrons that they form an equilibrium distribution given by (2), with η in (1) a function of time given by the cold electron dynamics, then we have the following simple picture for the build-up: For $\eta < \eta_m$, there is a flux of cold electrons into the ECRH zone $\Gamma = n_e(l, t)v_e$, where $v_e = (kT_e/2\pi m)^{1/2}$. Thus at $s = l$, we obtain

$$dn_h/dt = -dn_c/dt = (v_e/\pi w)n_c(l,t)S(l), \quad (5)$$

which yields

$$n_c(l,t) = n_{i0} \exp(-\alpha t), \quad (6)$$

where $\alpha = (v_e/\pi)(2/wl)^{1/2}$ is the rate of conversion of cold to hot electrons. The hot electron density and potential buildup are then given by

$$n_h(s,t) = n_{i0} (l/2w)^{1/2} (1 - e^{-\alpha t}) S(s), \quad (7)$$

and

$$\frac{\Phi(s,t) - \Phi(0,t)}{T_e} = \ln \left[\frac{n_i - n_h(s,t)}{n_i - n_h(0,t)} \right] \quad (8)$$

At $s = l$, $\Phi(l,t) = -\alpha T_e t$. Thus the steady state potential at the singularity point $s = l$ builds up linearly with time.

In addition to the heating of electrons originating in the ECRH cell there may also be some entry of electrons from regions external to the ECRH cell. For example, in the multiple-mirror experiment (MMX) there is a large reservoir of such electrons in other mirror cells. Since all electrons entering the resonance zone are (by definition) heated, this introduces excess electron charge into the ECRH cell which rapidly builds up an additional potential to essentially cut off this external flow. More exactly, the equilibrium requires a balance of flows of negative and positive charge species. The potential therefore adjusts itself to balance the electron flow into the cell against the loss of hot electrons and the ion flow into the cell. For strong heating, in which the characteristic change in electron energy in traversing the resonance zone is large compared to the initial electron temperature, the short time electron loss is negligible.⁸ Thus we expect a difference of potential of $\Phi(0) - \Phi_{ext} \sim -4 T_e$ to be rapidly established, to make external electron and ion flows into the cell equal. After the ECRH is turned off the Boltzmann distribution of the background cold electrons would be expected to reestablish itself throughout the device so that this potential difference rapidly collapses.

We now estimate w for a particular device with low initial temperature and high final temperature (the strong heating case). For ECRH heating in a quadratic well, the effective energy gain per pass through the resonance zone goes as⁹

$$\exp(-x^{2/3}), \quad (9)$$

where

$$x = \frac{\delta s}{L} \left[2 \frac{\omega}{v_{\perp}} L \right]^{2/3}, \quad (10)$$

δs is the distance from the turning to the resonance, and v_{\perp} is the perpendicular velocity at resonance. Thus $x = 1$ sets the scale length δs of the resonance zone. For the MMX experiment, to be considered in Sec. IV, we use the values $\omega = 2\pi \times 10^{10}$ rad/sec, $v_{\perp} = 2 \times 10^7$ m/sec ($E_{\perp} \approx 2$ keV) and $L = 0.3$ m to obtain, at $x = 1$, $\delta s = 0.23$ cm. Setting $L = l$ and $\delta s = w$, then from (4) we obtain $\eta_m = 0.2$, i.e., 20% of the electrons within $[-l < s < l]$ are heated.

We compare the δs obtained above with the penetration through the resonance Δs , due to the finite E_{\parallel} at resonance. Assuming $\mu = E_{\perp}/B$ and $E = E_{\perp} + E_{\parallel}$ to be constants in the turning (usual mirror assumptions), using the magnetic field gradient scale length $L = l/(R_0^{-1} - 1)$, where $R_0 = R(0)$ and assuming $\Delta s \ll l$, we have

$$\Delta s = \frac{l}{R_0^{-1} - 1} \frac{E_{\parallel}}{E_{\perp}}. \quad (11)$$

Taking $E_{\perp} \approx 2$ keV, $E_{\parallel} \approx 10$ eV and $L = 0.3$ m, as before, we find $\Delta s = 0.05$ cm, which is considerably less than the natural resonance width given by (10). We contrast this result with a tokamak example to be considered in detail in the next section. There, the initial electron temperature is of the order of 1 keV and the final temperature is of the order of 5 keV, with the scale length given by $l/(R_0^{-1} - 1)$ where $R_0^{-1} = 1.1$ from the aspect ratio. For those values, we have $w \approx \Delta s \approx 2l$ (the length of the mirror!) and $\eta_m > 1$, implying that all electrons are heated. However, for that case our approximations are not satisfactory, leading to the treatment given in the next section. The scale lengths are so different both because of the smaller mirror ratio and because of the higher background "cold" electron tempera-

ture.

III. Bi-Maxwellian Model

In this section we model the hot-electron distribution function as a bi-Maxwellian at the point along a field line where the ECRH is resonant:

$$f_h = C \exp [-(E_{\perp}/T_{\perp} + E_{\parallel}/T_{\parallel})] \quad (12)$$

where E_{\perp} and E_{\parallel} are the perpendicular and parallel energies at the resonance point, T_{\perp} and T_{\parallel} are perpendicular and parallel temperatures, and C is a normalization constant to be determined. The temperatures T_{\perp} and T_{\parallel} are prescribed in the present calculation, but in principle are determined by a competition between ECRH heating and collisions as well as the temperature of the initial electron distribution. Note that the connection between the results to be obtained with this model and those of Sec. II is via Eq. (11).

As in the preceding section we assume that the hot electrons are collisionless on the transit time scale so that the hot-electron distribution is everywhere given by (12) since E_{\perp} and E_{\parallel} are constants of motion (related to local variables through consistency of energy and magnetic moment). As in Sec. II we assume that hot electrons are sufficiently energetic to be unaffected by potential variations. Then the local hot-electron density is given by

$$\begin{aligned} n_h(s) &= \frac{4\pi R(s)}{m^2} \int \frac{dE_{\perp} dE_{\parallel}}{v_{\parallel}} f_h \\ &= \left[\frac{2T_{\parallel}}{m} \right]^{3/2} \pi R(s) \int_0^{\infty} d\varepsilon e^{-\varepsilon} \int_0^{\varepsilon_{\perp m}} \frac{d\varepsilon_{\perp}}{(\varepsilon - \varepsilon_{\perp} [1 - \lambda(1 - R(s))])^{1/2}} \end{aligned} \quad (13)$$

where $\lambda \equiv T_{\perp}/T_{\parallel}$, $\varepsilon_{\perp} = E_{\perp}/T_{\perp}$, and $\varepsilon = E_{\parallel}/T_{\parallel} + \varepsilon_{\perp}$. The range of ε_{\perp} integration has a maximum given by $\varepsilon_{\perp m} = \varepsilon$ for $R < 1$ and $\varepsilon_{\perp m} = \varepsilon/[1 + \lambda(R - 1)]$ for $R > 1$ (the difference being due to electrons at the resonance position which do not reach position s for $R > 1$). Hence we obtain

$$n_h = \left[\frac{2\pi T_{\parallel}}{m} \right]^{3/2} C \lambda g(R) \quad (14)$$

where

$$g(R) = \begin{cases} \frac{R}{1+[\lambda(1-R)]^{1/2}}, & R \leq 1, \\ \frac{R}{1+[\lambda(R-1)]}, & R \geq 1. \end{cases} \quad (15)$$

We normalize the hot-electron distribution so that the total number of hot electrons on a flux tube is a fraction η times the total electron number; this determines C so that

$$n_h = \hat{\eta} n_{e0} g(R) \quad (16)$$

with

$$\hat{\eta} = \frac{\eta}{\langle g \rangle} \quad (17)$$

and $\langle \rangle$ denotes a $\int ds/B$ average along a field line.

One may observe from (15) and (16) the expected peaking of the hot-electron density at the resonance position (where $g = 1$). One may also observe that, depending on values of λ and R , the maximum relative variation in hot-electron density occurs for heating at either the bottom or top of the magnetic well.

In contrast to the model discussed in Sec. II, the hot electron density is non-zero everywhere; however, for $\lambda \gg 1$, the density drops off rapidly with $R > 1$. As in Sec. II, on a time-scale short compared to ion transit times, the ion density is constant ($n_i = n_0$) and the cold Boltzmann electrons establish a potential variation along field lines

$$\frac{\Phi - \Phi_0}{T_e} = \ln \frac{n_i - n_h(s)}{n_i - n_h(s_0)} = \ln \frac{1 - \hat{\eta} g(R)}{1 - \hat{\eta} g(R_0)}, \quad (18)$$

where s_0 denotes some convenient reference point ($s_0 = 0$ in Sec. II).

The potential becomes singular at $R = 1$ when $\hat{\eta} = 1$. From (17) it follows that this always occurs for $\eta < 1$, as it can be seen from (10) that $\langle g \rangle < 1$. Thus, as in Sec. II, if the ECRH is on long enough the heating process extinguishes itself when less than all of the cold electrons are converted to hot; additional fueling can occur only on the time scale of the ion motion.

For the particular case of heating of the top of a sinusoidal well $B^{-1} \propto 1 + \delta \cos s/s_0$, a simple exact solution is obtainable. For this $B(s)$, we average $g(R)$ to obtain

$$\langle g \rangle = \begin{cases} \frac{4}{\pi} \frac{\arctan \left[\frac{1-K}{1+K} \right]^{1/2}}{(1-K^2)^{1/2}}, & K < 1 \\ \frac{2}{\pi} \frac{\ln \frac{1+\xi}{1-\xi}}{(K^2-1)^{1/2}}, & K > 1 \end{cases} \quad (19)$$

where $\xi = [(K-1)/(K+1)]^{1/2}$ and $K = (2\lambda\delta)^{1/2}$. Top-of-well heating is of interest for tokamaks because it minimizes trapped-particle effects on current drive and, as will be discussed in Sec. V, it minimizes toroidal variations of the ECRH-driven potential.

As in Sec. II, if the pulse is on for many hot-electron transit times, we can derive the approach to the logarithmically singular steady state described by (18) with $\hat{\eta} = 1$. The flux of cold electrons into the heating zone is $\Gamma = n_{er} v_e$, where n_{er} and v_e are the cold-electron density and the thermal speed at the resonance point. Hot electrons are created from this flux. These hot electrons spread themselves according to the weight function $g(R)$. Thus in the limit $n_h l / \tau_b \gg \Gamma$, where τ_b is the hot-electron bounce (or transit) time, the hot-electron density evolves as

$$\frac{dn_h}{dt} = \frac{\Gamma g(R)}{\langle g \rangle \int ds/R} \quad (20)$$

Since $n_e + n_h = n_i \equiv n_0 = \text{const}$, we have, as in Sec. II, exponential decay $n_{er} = n_0 \exp(-\alpha t)$, where now $\alpha = v_e / (\langle g \rangle \int ds/R)$. Thus we have the density

$$n_h(R, t) = g(R)(n_0 - n_{er}) = g(R)n_0(1 - e^{-\alpha t}) \quad (21)$$

and potential variation

$$\frac{\Phi - \Phi_0}{T_e} = \ln \frac{1 - g(1 - e^{-\alpha})}{1 - g_0(1 - e^{-\alpha})} \quad (22)$$

IV. Potential Evolution on Longer Timescales

As has been noted, the analyses of Secs. II and III become invalid for times of the order of ion transit times. On the ion transit timescale, the ions find themselves in the nonuniform potential set up by the (rapid) electron dynamics. Their distribution function when expressed in terms of constants of motion (total energy and magnetic moment) now has explicit spatial dependence. Consequently the ion density evolves in time, becoming spatially and temporally nonuniform, and taking on a sloshing character with oscillations on the ion-transit time scale. After several ion transit times, however, the ions phase mix and settle into an intermediate time-scale "quasi-steady-state" spatially nonuniform density which slowly changes on the ion or hot-electron collisional time scales. We approximately evaluate this phase-mixed state for heating at the top of a square well magnetic field. The model magnetic field and potential profiles, and the resultant trapped and passing regions in the ion velocity spaces, are sketched in Fig. 2. We assume that the ECRH heating pulse was on for a time short compared to the ion transit time scale. We assume that, before the ECRH pulse, the ion distribution function is Maxwellian $f_{Mi}(\mathbf{v})$, and that during the evolution of the potential, the distribution functions in the trapped portions of velocity space at the top and bottom of the well, expressed as functions of local velocity, do not change. Thus the final trapped-ion density n_{ij} in region j ($=1,2$) is given by $\int d^3v f_{Mi}(\mathbf{v})$ over the trapped portion of velocity space in region j . Taking note of the trapped ion boundary in cell 1 (see Fig. 2), $(v_{\parallel}/v)^2 = 1 - R^{-1} - \phi/R\varepsilon$, where $\varepsilon \equiv m v^2/2T_i$, $\phi \equiv \Delta\Phi/T_i$, and $R \equiv B_2/B_1$, we have:

$$\begin{aligned} n_{t1} &= n_0 \pi^{-3/2} v_i^{-3} \int_{trapped} d^3v \exp(-v^2/v_i^2) \\ &= 2n_0 \pi^{-1/2} \left\{ \int_0^{\phi} d\varepsilon \varepsilon^{1/2} e^{-\varepsilon} + \int_{\phi}^{\varepsilon_u} d\varepsilon \left[\frac{\phi}{R} - (1-R^{-1})\varepsilon \right]^{1/2} e^{-\varepsilon} \right\} \end{aligned}$$

where $\varepsilon_u = \phi/(1-R)$. These integrals can be expressed in terms of an error function and a Dawson integral,

$$n_{t1} = n_0[1 - \exp(-\phi)G_1(\phi)] \quad (23)$$

where

$$G_1(\phi) = e^\phi \exp(\phi^{1/2}) - 2 \left[\frac{1-R}{R\pi} \right]^{1/2} \text{Daw} \left[\frac{R\phi}{1-R} \right]^{1/2}$$

and the Dawson integral is defined as¹⁰

$$\text{Daw}(y) \equiv e^{-y^2} \int_0^y dt e^{t^2}.$$

Similarly the trapped density in cell 2 is

$$n_{t2} = n_0 \pi^{-1/2} \int_0^{\hat{\epsilon}} d\epsilon \epsilon^{1/2} e^{-\epsilon} + \int_{\hat{\epsilon}}^{\infty} d\epsilon \left[\epsilon^{1/2} - (1-R)^{1/2} (\epsilon - \hat{\epsilon})^{1/2} \right] e^{-\epsilon}$$

where $\hat{\epsilon} = R \epsilon_u$, or

$$n_{t2} = n_0[1 - G_2(\phi)] \quad (24)$$

where

$$G_2(\phi) = 1 - (1-R)^{1/2} \exp \left[-\frac{R\phi}{1-R} \right]$$

It follows that $(n_0 - n_{ij})\zeta_j$ ions from cell j become passing ions on the same flux tube, where $\zeta_j = L_j/B_j$ and L_j is the length of cell j . But we do not yet know how these are distributed axially. We determine this from the approximation that after phase mixing, the distribution function can be taken as Maxwellian in total energy (kinetic + potential) independent of axial position s . This approximation implies that $n_{pj} = \text{const} \times G_j$, where the constant is determined from the prescription that the total ion density be as given above,

$$\sum_j n_{pj} \zeta_j = \sum_j (n_0 - n_{ij}) \zeta_j$$

where the sum is over regions 1,2. Adding together passing and trapped densities, we obtain the final total ion densities

$$n_1 = n_0 \left\{ 1 + \frac{\zeta_2 G_1 G_2 (1 - e^{-\Phi})}{\zeta_1 G_1 + \zeta_2 G_2} \right\} \quad (25)$$

$$n_2 = n_0 \left\{ 1 - \frac{\zeta_1 G_1 G_2 (1 - e^{-\Phi})}{\zeta_1 G_1 + \zeta_2 G_2} \right\}. \quad (26)$$

The potential variation is then determined from quasineutrality. Assuming, as in Secs. II-III, that the hot-electron density is unaffected by the potential, we can use the hot-electron density found in Sec. III and thus obtain

$$\exp \frac{\Delta\Phi}{T_e} = \frac{n_2 - n_{h2}}{n_1 - n_{h1}} = \frac{n_2 - n_0 \hat{\eta} g(R)}{n_1 - n_0 \hat{\eta}} \quad (27)$$

As noted earlier this potential decays on the hot-electron and ion collisional time scales. If these time scales are disparate one may ask for the potential on the shorter time scale. If the hot-electron collision time is shorter, the potential decays to zero on that time scale. If the collision time is shorter, then on that time scale the ion density relaxes to a Boltzmann distribution,

$$n_i = \hat{n}_0 \exp(-\Phi/T_i)$$

where the normalization constant \hat{n}_0 is set by number conservation: $\hat{n}_0 = n_0 \langle \exp(-\Phi/T_i) \rangle$. The quasineutrality condition can be written in the form

$$\exp(\Phi/T_e) = \frac{\hat{n}_0 \exp(-\Phi/T_i) - \hat{\eta} n_0 g(R)}{\hat{n}_0 - \hat{\eta} n_0} \quad (28)$$

where we have defined $\Phi = 0$ at the resonance point. This is generally an integral equation for Φ . If we again introduce the square well approximation with heating at the magnetic field maximum, then we can write

$$\hat{n}_0 = \frac{n_0 (\zeta_1 + \zeta_2)}{\zeta_1 + \zeta_2 \exp(\Phi_i/T_i)}, \quad (29)$$

and (28) becomes an algebraic, though transcendental, equation for the potential Φ in region 2. Finally this potential decays on the hot-electron time scale.

The description given by (28) is also the appropriate one for steady-state potentials in a device with continuously heated electrons (where the electron collisional time scale is effectively infinite provided the steady-state hot-electron distribution function has been adequately modeled). The physics in this case is that of a steady-state tandem-mirror thermal barrier with ECRH heating and Maxwellian ions (no pumping).

V. Interpretation of MMX ECRH Experiment

Measurements of potentials created by short-pulse ECRH, in a single cell of a multiple-mirror device, have been made in the configuration shown in Fig. 3. Because of the short time-scale of the pulse, all measurements are made after the completion of the pulse, and are thus recording the fast-time scale equilibrium, before ions can move significantly, and the subsequent slower time scale evolution characteristic of the ion motion and collisional processes.

The experimental configuration, as shown in Fig. 3, consists of a quadrupole stabilized set of magnetic mirrors of length 75 cm with midplane fields of $B_0 = 0.18$ T. The central cell (with midplane at M_{67}), together with mesh-covered endplates at T_6 and T_7 having openings spaced to fit the elliptical flux surfaces, form a cavity for electron cyclotron resonance heating. A 3 μ sec, 250 kW, 9.0 GHz, rf heating pulse creates the magnetically confined, hot electron density n_h in this cell.

Diagnostics include Langmuir probes to measure plasma radial profiles, plasma density, and electron temperature in the mirror cells without hot electrons, an 8 mm microwave interferometer to measure the density in the cell containing hot electrons (the interferometer has been calibrated against a Langmuir probe measurement of the plasma density in M_{67} in the absence of ECRH), and high impedance emissive probes to measure plasma potentials. The temperature of the "tail" of the hot electron distribution is determined by measuring the x-ray flux in the 1-10 keV range using a cooled, Si(Li) detector with a beryllium window having 91 percent transmissivity at 2 keV. The total stored energy of the plasma is determined using a diamagnetic loop. The potential in the ECRH cell is measured using an electron beam time-of-flight diagnostic.^{4,5} A 100-200 volt, 0.5 mA, 1/8" diameter electron beam is injected in the midplane of cell M_{78} , propagates along the magnetic axis of the ECRH cell and is detected in the midplane M_{56} of the following cell. To determine the beam time-of-flight, the beam

current is modulated at a frequency of 10 MHz, and the phase delay of the signal received at the collector is measured.

In a typical experiment, the tail of the electron distribution was measured from pulse height analysis of the x-rays to be 2 keV. The total energy measurement from the diamagnetic loop, combined with the plasma density and profile measurements, gave an average hot electron energy, after the ECRH pulse, of $T_h \approx 770$ eV. Uncertainties in this latter measurement may be as much as a factor of two. In a previous study⁵ we took the electron distribution to be Maxwellian, with an average energy $T_h = 500$ eV. The decay of the hot electrons at this temperature, together with a smaller effect due to the trapping of ions in the ECRH cell, gave good agreement with the measured decay in the potential in the ECRH cell, as shown in Fig. 4. Although not specifically discussed in the previous paper, the choice of $T_h = 500$ eV, together with the diamagnetic loop and x-ray measurements, implies a two-temperature distribution. Taking the hotter component to have a temperature of 2 keV (from the x-ray pulse height analysis) and the averaged temperature to be 770 eV (from the diamagnetic signal and average density), then energy conservation implies that slightly under 20 percent of the electrons are heated to the higher energy. This result is consistent with our calculations in Sec. II which indicate that about 20 percent of the electrons can be heated to the characteristic ECRH energy before the buildup of the potential excludes the remaining electrons from entering the main heating zone. Further details regarding the experiment and its interpretation can be found in reference 5.

VI. Application to MTX

We consider application of the results of Secs. III and IV to a tokamak heated by pulsed ECRH, such as the MTX experiment⁶ to be constructed at Lawrence Livermore National Laboratory. MTX consists of the ALCATOR-C tokamak plus a free-electron maser (FEM). The FEM produces 100 to 200 joule pulses of duration $\tau_p = 50$ ns with a 5 kHz repetition rate. The microwaves will enter the plasma as a beam of rectangular cross section of about 4 cm \times 20 cm. The r.f. field is sufficient to raise the perpendicular energy of a 1 keV electron to as much as 10 keV on a single pass through resonance.

We consider application of the FEM to an MTX plasma with a density of 10^{14} cm^{-3} and a range of background electron temperatures T_e . We evaluate the hot-electron anisotropy $\lambda \equiv T_{\perp} / T_{\parallel}$ by taking $T_{\parallel} = T_e$ and T_{\perp} to be half the maximum amplitude of the energy oscillations of electrons in the intense microwave field.^{6,10} From Refs. 6 and 10, this implies, for fundamental ordinary-mode heating in MTX, $\lambda \sim 5 T_e^{-2/3} (\text{keV})$. The pulse duration limits the hot-electron fraction to about the ratio of τ_p to the mean electron toroidal transit time, giving $\eta \equiv 0.25 T_e^{1/2} (\text{keV})$. Since ion transit times, which are about 10^{-4} sec at 1 keV, are long compared to the pulse length and electron transit times, it is appropriate to apply the potential calculations of Secs. III and IV. For heating on the inside of the flux surface (at the field maximum) at $\delta \equiv \text{minor radius/major radius} = 0.1$, we find from (17)-(19) that, on the hot-electron transit time scale ($\sim 10^{-7}$ sec) the potential variation is as shown by the curve labeled "e" in Fig. 5. We note that the expected range of electron temperatures is about 1-2 keV, the lower figure being the value obtained in ohmic ALCATOR-C discharges. Over this range, $\Phi/T_e \approx 0.3-0.4$. Results at lower T_e are relevant to startup. Note that Φ/T_e increases with increased T_e ; this is because the increase in the hot-electron fraction (due to the increased number of electrons passing through the microwave beam during the time τ_p) more than compensates for the decreased anisotropy. As T_e approaches about 10 keV, the calculated potential diverges due to the choking off of the flow of cold electrons as described in Secs. II and III. However, because T_{\perp} is not extremely large compared to the computed potential, our calculation, which assumes that the hot electrons are unaffected by the potential, is of doubtful validity beyond $T_e \approx 4 \text{ keV}$.

On the time scale of several ion transits, the potential relaxes to that given by the curve labeled "it" in Fig. 5, i.e., $\Phi/T_e \approx 0.2$ for T_e in the range of 1-2 keV. This curve was obtained using (27) with $\zeta_1 = \zeta_2$, and $T_i = T_e$.

For completeness we note that, were the hot-electron time scale and inter-pulse period long compared to the ion-collision time (which is not the case), or were we to maintain a hot electron fraction and anisotropy equal to those discussed above by continuous heating (which could happen only if hot electrons were lost in a time short compared to their relaxation time) the potential would, on the ion-collision time scale, settle down to the values given by the curve labeled "ic" in Fig. 5. This is

obtained from (28) and (29), again with $\zeta_1 = \zeta_2$ and $T_i = T_e$.

VII. Discussion and Conclusion

The application of intense, short pulses of ECRH to a plasma in a nonuniform magnetic field can generate sizable potentials on the transit time scale of the heated electrons. These potentials can affect the heating process itself to limit the fraction of the electrons heated. A negative potential is formed by the sloshing hot electrons in the presence of transiting cold electrons which form a Boltzmann distribution along the field lines. The potentials relax to successively smaller values on the ion-transit and ion-collision time scales and decay on the hot-electron collisional time scale. The same mechanism forms potentials in continuously heated plasmas, but typically at much smaller levels, because the hot-electron anisotropy is much smaller.

We investigated the shape and magnitude of the potential profile in for two different distributions of hot-electron turning points. First, in Sec. II, we assumed that the hot-electron turnings were uniformly distributed over a width determined from the ECRH dynamics. Second, in Sec. III, we assumed that the hot-electron distribution function is bi-Maxwellian, yielding a non-uniform turning distribution.

In confinement devices with a sufficiently large combination of mirror ratio and hot electron anisotropy (sufficiently strong heating), both formulations predict that the flow of cold electrons from within the mirror into the heating zone is effectively shut off by the potential build-up after only a small fraction of the electrons are heated. This prediction was compared with the experimental observations of electron heating in a short-pulse ECRH experiment, MMX, and found to be consistent with them.

The potential structures we have calculated are fundamentally variations along field times. However, if the microwave source is localized in directions transverse to field lines, there may be potential variations in those directions as well. Of particular interest are axisymmetry-breaking potential variations (toroidal in a tokamak, azimuthal in a mirror), as such variations are likely to significantly enhance neoclassical transport. Consider a tokamak with a toroidally localized microwave source. To the extent that the hot electrons are all passing (this is most true for heating resonant on the inside of the flux surface) then on an irrational flux surface, the hot electrons distribute over the entire flux

surface, producing only a poloidal density and hence potential variation. Trapped hot electrons can fill the flux surface only on the (slow) drift time scale. If this time scale is comparable to or longer than hot-electron and ion collision times (as is the case for MTX), the potential must vary toroidally as well as poloidally. Heating on a flux surface with resonance not at the inside directly produces trapped hot electrons. Even for resonance at the inside, the combination of cyclotron heating and collisions produce some trapped hot electrons. Thus there will always be some toroidal potential variation, but it can be minimized (on irrational surfaces) by heating at the field maximum. On a rational surface, a field line does not cover the flux surface; hence, in the neighborhood of a rational surface, potential variation is confined to field lines which pass through the microwave beam, so that the potential takes on a helical structure.

The presence of these potentials can have other consequences. One is parametric coupling of the time-varying potential to low-frequency modes of the plasma. Difficulties associated with such coupling might be avoided by changing the repetition rate. A conceivably beneficial effect is enhanced heating. On the ion-transit time scale, ions flowing into the potential wells set up by the hot electrons are accelerated, which, for large $\Delta\Phi/T_i$, may result in a two-stream instability and thus lead to rapid energy transfer from the passing to the trapped ions. For smaller potentials the streaming and background ion populations equilibrate on an ion-ion scattering time scale. Either mechanism provides a faster process of converting hot-electron energy to ion energy than direct electron-ion energy equilibration.

Acknowledgement

Research sponsored by the Department of Energy Grant DE-FGO3-86ER51103 and Department of Energy Contract W-7405-ENG-48.

References

- ¹D. E. Baldwin and B. G. Logan, *Phys. Rev. Lett.*, **43**, 1318 (1979).
- ²T. Uckan, L. A. Berry, D. L. Hillis, and R. K. Richards, *Phys. Fluids*, **25**, 1253 (1982).
- ³H. D. Price, H. R. Garner, and RFC XX Team, *Nuclear Fusion*, **26**, 611 (1986).
- ⁴J. C. Fernandez, C. P. Chang, A. J. Lichtenberg, M. A. Lieberman, and H. Meuth, *Phys. Fluids*, **29**, 1208 (1986).
- ⁵C. P. Chang, M. A. Lieberman, H. Meuth, and A. J. Lichtenberg, "Observation of a Potential Barrier Created by Electron Cyclotron Resonance Heating in a Multiple Mirror Plasma," submitted to the *Physics of Fluids* (1986).
- ⁶K. I. Thomesson, Ed., "Free Electron Laser Experiment in ALCATOR C," LLL-PROP-00202, Lawrence Livermore National Laboratory (U.S. Government Printing Office 1986-8-687-002/44101), July 1986.
- ⁷A. J. Lichtenberg and C. Melin, *Phys. Fluids*, **16**, 1660 (1973).
- ⁸F. Jaeger, A. J. Lichtenberg, and M. A. Lieberman, *Plasma Phys.*, **14**, 19073 (1972).
- ⁹M. Abramowitz and I. Stegun, *Handbook of Mathematical Functions* (Dover, New York, 1972) p. 298.
- ¹⁰W. M. Nevins, T. D. Rognlien, B. I. Cohen, "Nonlinear Limits on Electron Heating with Intense Microwave Pulses," Lawrence Livermore Laboratory Report UCRL 95006 (1986), submitted to *Physical Review Letters*.

FIGURE CAPTIONS

- Fig. 1. (a) Normalized hot-electron density $S(s)$ and (b) potential $\Phi(s)$ versus axial position s .
- Fig. 2. Square well model (a) and ion velocity distribution function boundaries (b) for determining the potentials on ion transit timescales.
- Fig. 3. MMX experimental configuration, including a schematic (not to scale) of two magnetic field lines 180 degrees apart. The mirror midplanes (M) and throats (T) are indicated.
- Fig. 4. Spatially average barrier depth $\langle\Phi\rangle/T_e$ vs time t for a medium diamagnetic loop voltage discharge. The solid line is the simulation result and the crosses give the measured result, with the height of each cross indicating the standard deviation of the phase delay measurement.
- Fig. 5. Expected potential buildup of $\Delta\Phi = \Phi(B_{\max}) - \Phi(B_{\min})$ versus cold electron temperature T_e for the MTX experiment, on the (e) hot-electron transit timescale, (it) ion transit timescale and (ic) ion collisional timescale.

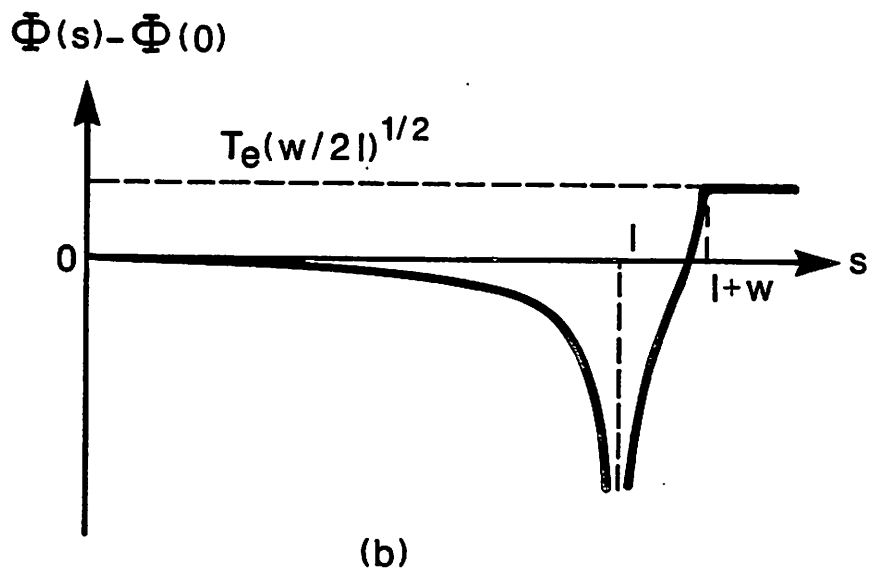
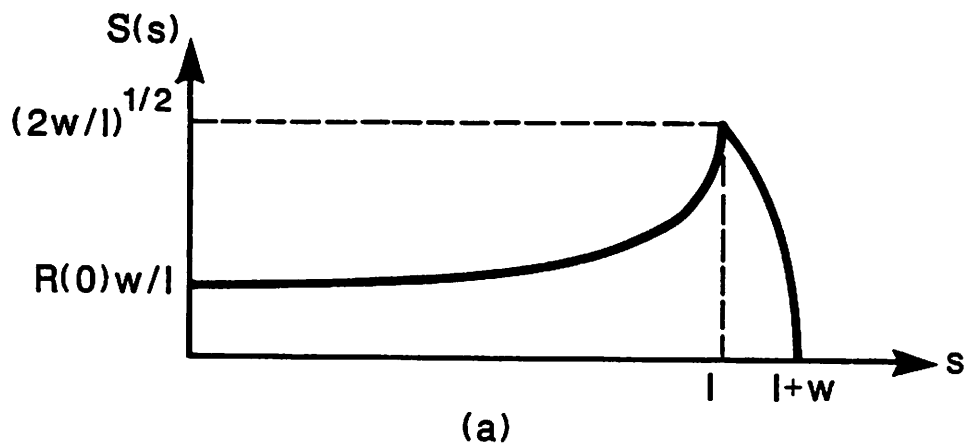


Figure 1

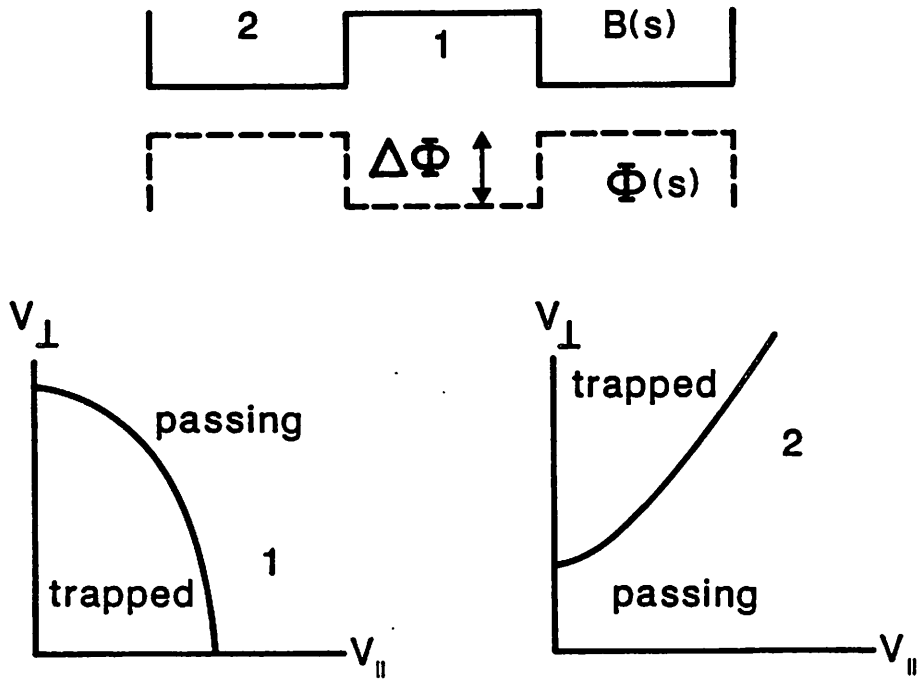


Figure 2

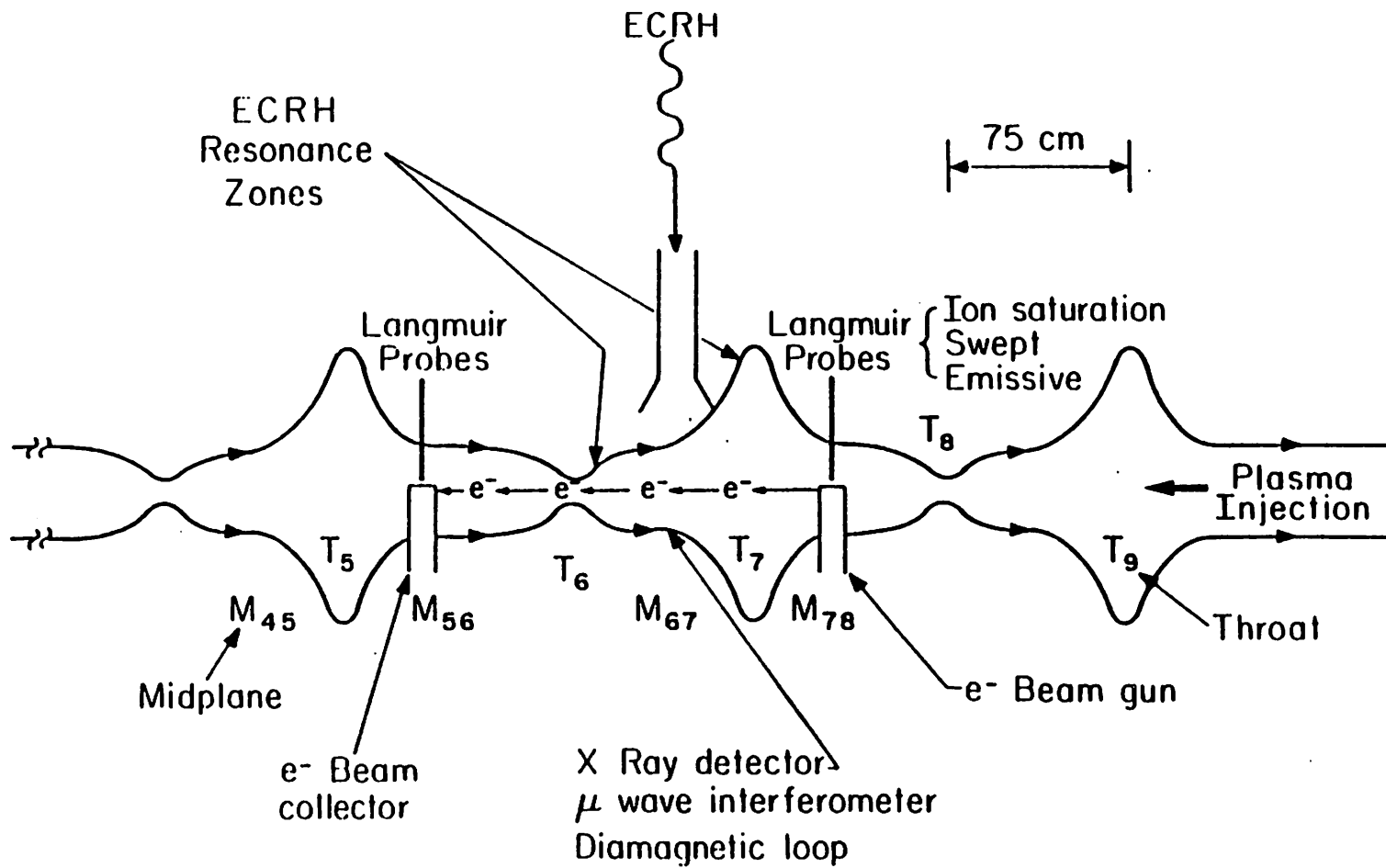


Figure 3

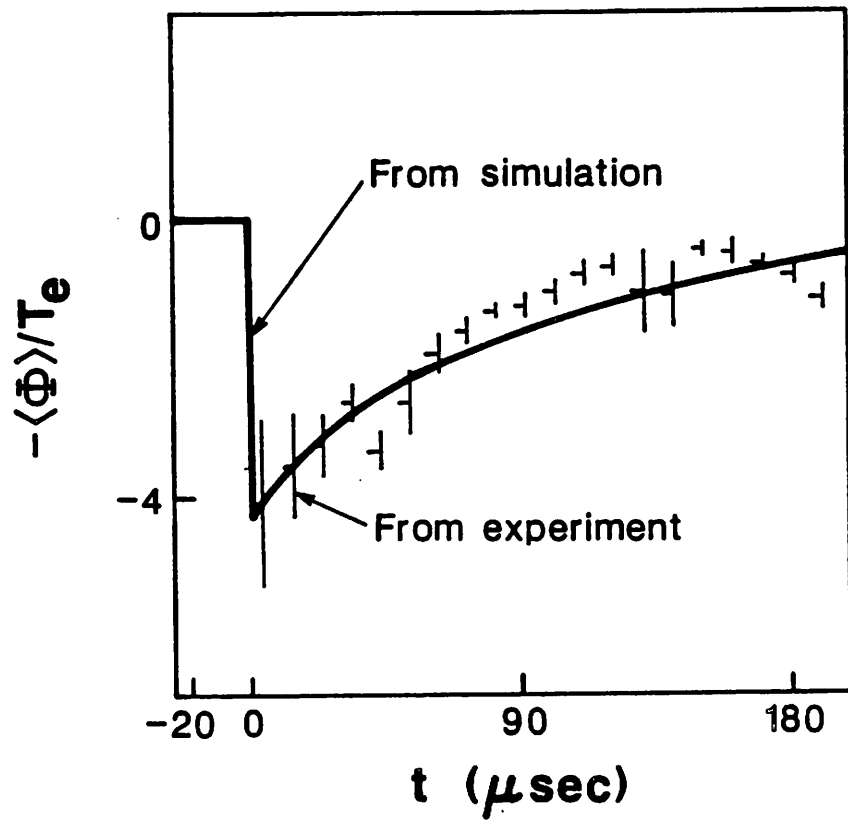


Figure 4

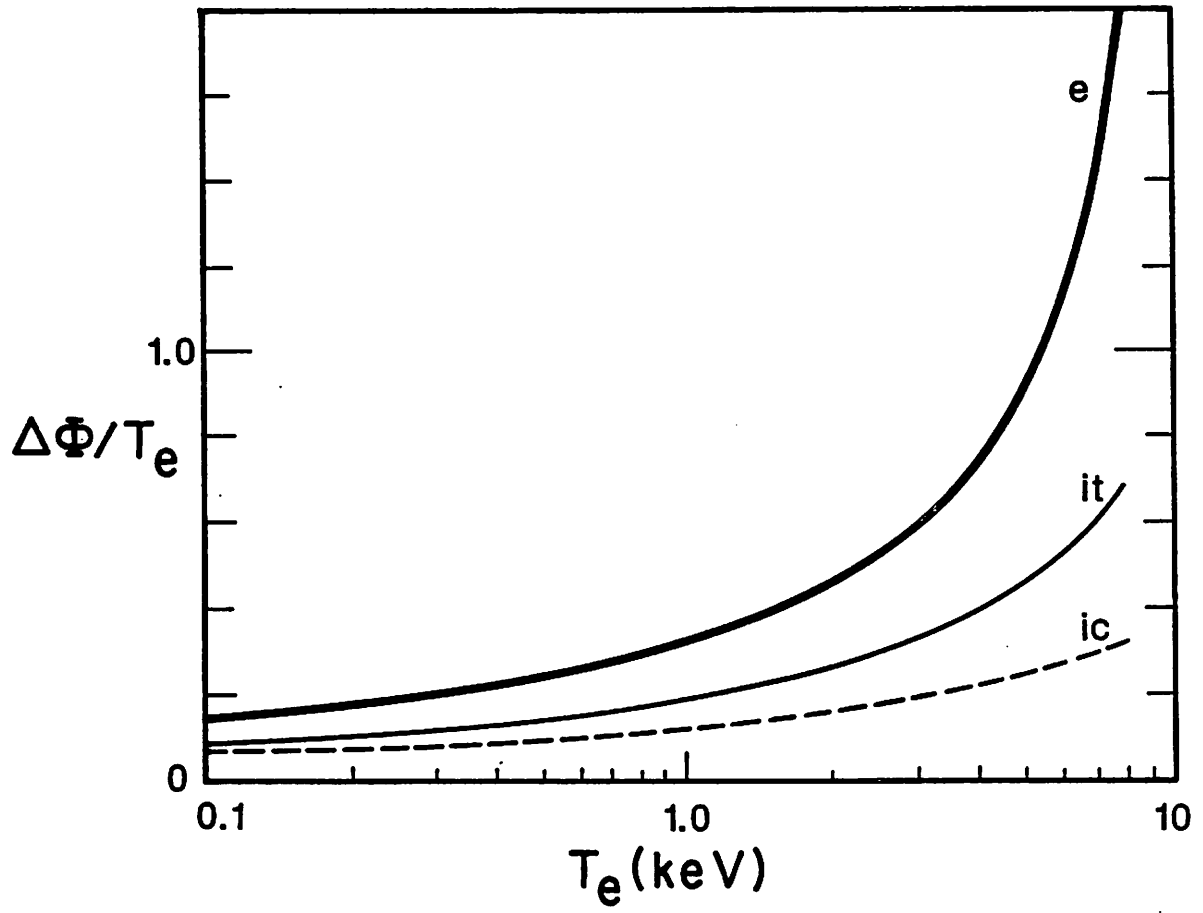


Figure 5